# OMAE2025-152685

# THE IMPACTS OF LONG-TERM SUBMERSION IN SEAWATER ON THERMOPLASTIC-MATRIX COMPOSITE MATERIALS

Ione L. M. Smith<sup>1,2</sup>, James M. Maguire<sup>3,4</sup>, Machar Devine<sup>4</sup>, Edward D. McCarthy<sup>1,4</sup>, Philipp R. Thies<sup>5</sup>, Selda Oterkus<sup>6</sup>, Winifred Obande<sup>4,\*</sup>

<sup>1</sup>EPSRC and NERC Industrial CDT in Offshore Renewable Energy (IDCORE), Edinburgh, United Kingdom

<sup>2</sup>FastBlade, Rosyth, United Kingdom

<sup>3</sup>The University of Sheffield, Sheffield, United Kingdom

<sup>4</sup>The University of Edinburgh, Edinburgh, United Kingdom

<sup>5</sup>University of Exeter, Penryn, United Kingdom

<sup>6</sup>University of Strathclyde, Glasgow, United Kingdom

#### **ABSTRACT**

Tidal turbine blades operate under challenging conditions as integral components of tidal energy converters. Constant submersion in seawater and exposure to high loads necessitate thick wall sections (10–100 mm) throughout blades, particularly at the root. Thermoset matrices are conventionally used in vacuum infusion processing to form durable fibre-reinforced composite components with structural integrity. However, the cross-links that provide these desirable properties also prevent melting and reshaping, limiting recyclability compared to thermoplastics. Advancements in recyclable liquid thermoplastic resins (LTPR) offer the opportunity for more sustainable material solutions for composite blades. Understanding the effects of prolonged submersion in saltwater on LTPR composite materials is critical for their application in thick-section structures used in the marine and tidal energy industries. This paper investigates the water uptake of two glass fibre/LTPR composites, manufactured with different grades of the same acrylic-based resin, Elium® 188 XO and Elium® 191 XO/SA, using accelerated ageing testing to simulate 10 years of submersion. GF/Elium® 191 XO/SA reached saturation more rapidly than GF/Elium® 188 XO, resulting in a greater total mass increase of 1.00% compared to 0.54%, with standard deviations of 0.65% and 0.02%, respectively. This study is part of an ongoing, longer-term assessment aimed at experimentally simulating a 20-year lifespan, representing the full design life of tidal turbine blades.

Keywords: Turbine Blades, Materials, Composites, Thermoplastics, Thick-section, Vacuum infusion processing, Water absorption

#### **NOMENCLATURE**

Acronyms and Material Designations

CF	Carbon fibres
EOSL	End-of-service-life
E188 XO	Elium <sup>®</sup> 188 XO
E191 XO/SA	Elium® 191 XO/SA
FRC	Fibre-reinforced composite

GF Glass fibres

LTPR Liquid thermoplastic resin SSE Sum of squares error

Latin Letters

 $D_z$  Diffusion coefficient [m<sup>2</sup>s<sup>-1</sup>] h Average specimen thickness [mm]

M(t) Moisture content of material as a function of

time, % of oven-dry mass

 $M_m$  Moisture equilibrium content of material, % of

oven-dry mass

 $T_g$  Immersion time [seconds]

Glass transition temperature [°C]

 $V_b$  Specimen baseline mass before submersion [g]

 $W_i$  Specimen mass at time of weighing [g]

#### 1. INTRODUCTION

Tidal energy has considerable potential as a reliable renewable energy resource. It is predicted that by 2050, the UK's electricity demand will rise to between 550 and 680 TWh/year, compared to 317 TWh in 2023 [1, 2]. The UK's practical tidal energy resource is estimated at 34 TWh/year, which accounts for 50% of Europe's resources [1, 3]. Rotor blades are a key component of tidal energy converters such as tidal stream turbines. Continuously submerged in saltwater, tidal turbine blades

<sup>\*</sup>Corresponding author: w.obande@ed.ac.uk

are continually subjected to high loads, necessitating the use of thick sections (10-100 mm), especially in the root of the blade [4, 5].

The majority of tidal turbine blades are manufactured from thermoset polymer fibre-reinforced composite (FRC) materials using vacuum infusion processing, reinforcing an epoxy matrix with glass fibres (GF) or carbon fibres (CF) [4–9]. Thermoset FRCs have traditionally been the preferred material choice for composite applications because of their ease of manufacturing, good mechanical properties, environmental resistance, and low cost. Despite their relatively superior toughness, impact resistance and out-of-plane properties, thermoplastics are typically melt-processed and therefore solid at room temperature and therefore require high temperatures and pressures during manufacturing limiting their applicability [10–12].

The cross-links in thermosets provide the durability and structural resilience needed for tidal turbine blade parts, but this same cross-linking typically prevents melting and reshaping — characteristics essential to many conventional recycling processes accessible to thermoplastics. Since there are currently no large-scale recycling solutions for managing decommissioned turbine blades, blades are incinerated or disposed of in landfill if not repurposed. Presently, the waste generated by the tidal energy industry is relatively minimal due to the limited number of deployed devices, many of which have not yet reached their end-of-service-life (EOSL). However, it is estimated that 1 GW of tidal energy capacity will result in around 6,000 tonnes of blade waste. With projections indicating 0.9 GW of installed tidal capacity in the UK by 2035, the potential for waste generation is significant and cannot be ignored [13, 14].

Recent material innovations in recyclable liquid thermoplastic resins (LTPR) provide the potential for more sustainable material choices for composite blades [6–9, 15, 16]. These materials are initially low-viscosity resins that can be processed at low, ambient temperatures using established resin infusion techniques to produce parts with high strength, toughness and impact resistance, making them a potential direct replacement for epoxy resins[10, 15, 17, 18]. A key factor in assessing the suitability of these materials for thick-section structures commonly used in the marine and tidal energy sectors is their water absorption behaviour over the product's lifetime.

Water absorption in FRCs is associated with both physical and chemical changes in materials, including reduced mechanical properties, swelling, shape deformation and hydrolysis [19–21]. The swelling and plasticisation of the matrix in acrylic-based FRC materials as a result of water uptake are known to lead to a decrease in mechanical properties and degradation of the fibre-matrix interface [18]. Within the same environment, the rate of diffusion and amount of water absorbed by FRC materials is dependent on multiple factors including the type of resin and fibres, fibre volume fraction, fibre:matrix interface and the material microstructure including any cracks or defects [20, 22–24]. The harmful impacts of water ingress on FRC tidal turbine blades can be mitigated by further increasing the thickness of parts, which introduces additional design and manufacturing challenges [24].

Previous studies have investigated the diffusion kinetics of acrylic LTPRs submerged in seawater, assessing unreinforced acrylic LTPR samples, as well as those reinforced with carbon or glass fibres [18, 22]. However, there has been little focus on the behaviour of these materials in thick-section laminates for an extended test period. The objective of this paper is to evaluate the long-term behaviour of two acrylic-based, thick-section FRCs in seawater through accelerated ageing testing. This study is part of an ongoing assessment to experimentally simulate a 20-year period, which represents the full target design lifetime of tidal turbine blades. This paper focuses on the first 10 years of testing, presenting conclusions from this initial phase and outlining directions for future work.

The remainder of this paper is structured as follows: the materials and experimental methods are introduced in Sect. 2, including the diffusion models considered. Section 3 presents the results and discussion, as well as an outline of the ongoing, longerterm assessment and future work. Finally, the paper concludes in Sect. 4.

#### 2. MATERIALS & METHODS

#### 2.1 Materials

This work compares two distinct grades of acrylic-based LTPR, Elium® 188 XO (E188 XO) and Elium® 191 XO/SA (E191 XO/SA), which polymerise in-situ when combined with an initiator. Both grades are low-exotherm variants for use in infusion processing, specifically for applications in the marine and wind industries where thick-section composite components are commonly used. The properties of the two resins are summarised in Tab. 1 [15, 25, 26].

TABLE 1: COMPARISON OF UNREINFORCED LOW-EXOTHERM ACRYLIC LTPR GRADES USED IN THIS STUDY [27, 28].

Property	E188 XO	E191 XO/SA
Viscosity	100	100
(cP at 25°C)		
Processing temperatures	20 - 60	20 - 60
(°C)		
Reactivity	60 - 90	> 60
(minutes)		
Initiator	BP-50-FT peroxide	MEKP Butanox M50
	United Initiators	Easy Composites
Additional information	DNV certified	-
Water uptake -		
7 days at 23°C (ISO 62)	0.55%	0.86%

One laminate was created from each resin, combining the LTPR with ten plies of quasi-unidirectional (quasi-UD) E-glass fibre (GF) fabric, which contains an acrylic-specific sizing agent (Textile Structure 7009444; Johns Manville & SAERTEX). The quasi-unidirectional (quasi-UD) non-crimp fabric comprised 0° fibres (1152 g/m²), 90° fibres (35 g/m²), and synthetic polyester stitching (13 g/m²) for a total areal weight of 1200 g/m²). Each laminate was manufactured using 3 parts initiator to 100 parts resin by weight, with a five-minute mix time. Peroxide initiator BP-50-FT (United Initiators) was used for the E188 XO laminate and methyl ethyl ketone peroxide (MEKP) catalyst (Easy Composites) for E191 XO/SA.

#### 2.2 Laminate Fabrication

In the production of tidal turbine blades, dry fibres are arranged into a single-sided mould. Manufacturing aids, such as distribution medium and peel ply, are placed on top, and a vacuum bag is applied to serve as the upper mould half. The vacuum facilitates the continuous flow of resin over the layup. This process is often referred to as Vacuum Assisted Resin Transfer Moulding (VARTM) in the context of tidal turbine blade manufacture [16, 29].

In this study, a glass plate covered with release film was used as the tool for the vacuum infusion. An infusion medium, serving as both flow mesh and perforated release film, was positioned on the tool before laying the glass fibre fabric and another layer of infusion medium. While the use of flow mesh on top of the layup is standard practice, the extra layer between the layup stack and and the tool was used to enhance resin flow through the thick laminate. It should be noted that, for both layers, the infusion medium was slightly narrower and shorter than the laminate to prevent resin race tracking. Each ply measured 195 mm x 460 mm x 10-plies equating to polymerised thicknesses of 8.4 mm and 7.8 mm for the GF/E188 XO and GF/E191 XO/SA laminates respectively.

# 2.3 Sample Preparation

Samples were taken from each panel using water jet cutting. For each material, four samples, each measuring 100 x 100 mm, were obtained for water ageing testing. The surface finish of the entire laminate varied in certain areas. For example, imprints were present where the resin inlet port was located on each laminate, as well as in areas intentionally not covered by infusion media. The position of the samples on the plate was optimised to maximise space, ensuring even thickness distribution and consistent surface quality for each specimen, as demonstrated in Fig. 1.

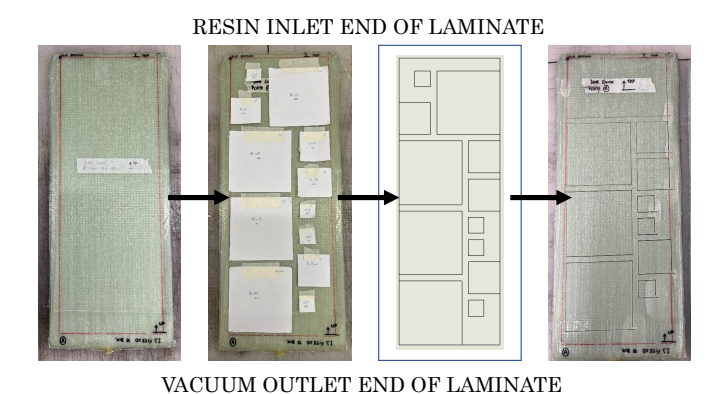


FIGURE 1: FOUR 100 X 100 MM SPECIMENS WERE CUT FROM EACH LAMINATE USING WATER JET MACHINING.

The thickness of the laminates posed challenges for sample extraction, as standard tools such as sawing and milling would cause excessive damage to the laminate sheet. Water jet cutting was selected since it presented the lowest risk to laminate quality. However, slight delamination was evident at the corners of some samples where the jet entered the laminate. On inspection,

two of the GF/E188 XO samples sustained minor damage, and one GF/E191 XO/SA sample was severely damaged as shown in Fig. 2. Typical issues in composite laminate manufacturing, such as incomplete fibre wetting, inadequate ply consolidation, and trapped air, are amplified in the production of thick-section laminates. These challenges can result in void formation, uneven polymerisation, and reduced dimensional stability throughout the laminate's thickness. Some level of variation between samples of the same material and presence of defects was therefore expected. Surface level voids and cutting-induced delamination defects visible by eye were noted prior to immersion.

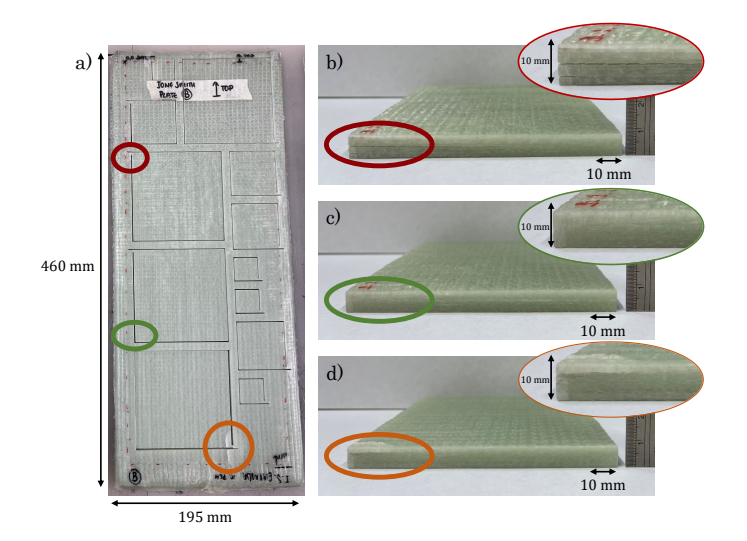


FIGURE 2: EVIDENCE OF CUTTING-INDUCED DELAMINATION ON GF/E191 XO/SA LAMINATE PLATE (A), WITH SOME RESULTING DEFECTS CLASSED AS MAJOR (B) AND SOME AS MINOR (D). SOME SAMPLES REMAINED UNAFFECTED (C).

ASTM D5229/D5229M specifies that specimens for thicklaminates with anisotropic moisture diffusivity constants should measure 100 x 100 mm with either aluminium or stainless steel bonded to the edges [30]. This is to minimise edge effects and ensure water is absorbed through the thickness of the laminate rather than along the fibres. No adhesive with a specified hydrophobic nature that could withstand the test temperatures in saltwater was available on the market at the time of sample preparation, meaning any adhesive used would be prone to water absorption. The authors understand that other studies have encountered issues with metal plates detaching during testing. Metallic plates would also corrode in the saltwater, introducing unknowns to the experiment. Painting and leaving only the top and bottom faces of the laminates exposed to ensure through-thickness water absorption was considered. However, there were concerns that surface preparation of the samples for painting might render the edges of the laminate hydrophilic. The edges of the samples were therefore left in their as-cut state. This is considered the worst case test environment for a tidal turbine blade, which would have a coating and paint protecting the FRC from seawater, with water only coming into contact in the case of damage or a defect in the surface finish.

### 2.4 Seawater Ageing

This study forms part of an ongoing longer-term assessment using accelerated ageing to simulate a 20-year period, the target lifetime of a tidal turbine blade, as discussed in Sect. 1. Samples are submerged in filtered natural seawater at  $55^{\circ}$ C ( $\pm 2.5^{\circ}$ C) and this paper considers data up to almost seven months submersion, replicating 10 years at 9°C sea temperature, outlined in Appendix A. It is generally recommended that the test temperature of seawater ageing experiments is at least 20°C below the glass transition temperature of the material,  $T_g$ . However, studies have shown that  $T_g$  of a material can reduce by around 20°C for every percentage increase in moisture and ASTM D5229/D5229M recommends to keep material samples 25°C below the wet  $T_g$ [30, 31]. The  $T_g$  for GF/Elium<sup>®</sup> composites has been found to exceed 100°C and is specified as 102°C for cured, non-reinforced resin by Arkema [22, 27, 32]. 55°C was therefore selected as the test temperature as it provides a suitable ageing acceleration factor without degrading the polymer matrix [19, 31, 33, 34].

Seawater was collected from Longniddry, Scotland, and filtered using aquarium wool to remove sediment before being heated in a water tank. Evaporated water is periodically replaced with distilled water to ensure the salinity and volume of water remains constant. Samples were oven-dried at 50°C for 17.5 days prior to immersion. Each sample is held in a bag made from infusion mesh, mounted within the tank using fishing wire to ensure all sides of the samples are exposed to water, as shown in Fig. 3. A circulation pump is used to continually agitate the water.

Thermocouple for temperature control

Water pump for circulation

Heating element

Material samples in mesh bags

FIGURE 3: SEAWATER AGEING TEST TANK SHOWING SAMPLES SUBMERGED IN WATER (SHOWN WITHOUT TANK LID FOR CLARITY).

At each measurement interval, samples were removed from the test tank and placed in buckets of tap water for 15 minutes to cool. Lint-free cloths were then used to pat dry all faces of each specimen, removing any surface moisture. Each specimen was weighed using a mass balance with a readout and reproducibility of 1 mg. Samples were weighed in batches, and the measurement procedure for GF/E191 XO/SA samples began 15 minutes after GF/E188 XO, ensuring samples were out of the test tank for less than 30 minutes, as specified in ASTM D5229/D5229M.

The percentage mass increase was calculated at each weighing interval, M(t), using Eq. 1 ([30]) where  $W_i$  is the specimen

mass at time of weighing and  $W_b$  the baseline dry mass of the sample before submersion. The average of the four samples for each material group was calculated at each timestamp and used for analysis.

$$M(t) = \frac{W_i - W_b}{W_b} \times 100 \tag{1}$$

#### 2.5 Diffusion Models

Diffusion coefficients,  $D_z$ , and moisture equilibrium content,  $M_m$ , of samples can be calculated using Fickian diffusion models as outlined in ASTM D5229/D5229M [30]. In order for a material to be classed as Fickian, absorption and desorption curves plotted on a graph of  $M_m$  versus  $\sqrt{time}$  must be essentially linear up to 60% of  $M_m$ , and then exhibit a concave portion relative to the x axis until  $M_m$  is reached. For the same testing conditions, absorption curves for different thicknesses of the same material must be super-imposable if the x axis is plotted  $\sqrt{time/thickness}$  as opposed to  $\sqrt{time}$  [30]. Equation 2 can be used to fit a Fickian diffusion curve to data, enabling calculation of  $D_z$  and  $M_m$  for material test specimens of thickness, h [18, 30].

$$M(t) = \left( M_m \left\{ 1 - \exp\left[ -7.3 \left( \frac{D_z t}{h^2} \right)^{0.75} \right] \right\} \right)$$
 (2)

There are material forms that are known to invalidate these assumptions, potentially resulting in non-Fickian behaviour. This may include materials with a multi-phase diffusion mechanism, notable surface cracking, an unusually high number of voids, or uneven void distribution amongst other reasons [30]. Dual Fickian diffusion models have been used to interpret non-Fickian behaviour in cases where two diffusion processes occur simultaneously, each with distinct speeds and maximum moisture capacities. Equation 2 is therefore expanded to form Eq. 3. This enables calculation of two different diffusion coefficients,  $D_{z1}$  and  $D_{z2}$ , and moisture content values,  $M_{m1}$  and  $M_{m2}$ , that correspond to each diffusion process, the sum of which gives the total moisture saturation as shown in Eq. 3 [35, 36].

$$M(t) = \left( M_{m1} \left\{ 1 - \exp\left[ -7.3 \left( \frac{D_{z1}t}{h^2} \right)^{0.75} \right] \right\} \right) + \left( M_{m2} \left\{ 1 - \exp\left[ -7.3 \left( \frac{D_{z2}t}{h^2} \right)^{0.75} \right] \right\} \right)$$
(3)

#### 3. RESULTS & DISCUSSION

Figure 4 shows the percentage mass increase versus the square root of immersion time for the GF/E188 XO and GF/E191 XO/SA specimens. An initial analysis of the plotted experimental data suggests that both materials exhibit Fickian behaviour, displaying a linear increase in water uptake followed by a plateau upon reaching saturation. However, when calculating the best-fit curve, a Dual Fickian model yielded a lower sum of square errors (SSE) value for both material sets, suggesting that the material forms analysed invalidate one of the assumptions of Fickian diffusion outlined in Sect. 2.5. Values presented are therefore the

average of each of the four specimens and the plotted curve of best fit was calculated using a Dual Fickian diffusion model using Eq. 3. Figure 3 also displays the minimum and maximum measured values for each material group. The resulting diffusion coefficients,  $D_{z1}$  and  $D_{z2}$ , and moisture content values,  $M_{m1}$  and  $M_{m2}$ , are presented in Tab. 2.

TABLE 2: DIFFUSION COEFFICIENTS,  $D_z$ , AND EFFECTIVE MOISTURE EQUILIBRIUM CONTENT,  $M_m$ , OF GF/E188 XO AND GF/E191 XO/SA SAMPLES AT 55°C. VALUES CALCULATED USING A DUAL FICKIAN DIFFUSION MODEL.

	GF/E188 XO	GF/E191 XO/SA
$D_{z1} (m^2 s^{-1})$	$1.02 \times 10^{-9}$	$1.30 \times 10^{-10}$
$D_{z2} (m^2 s^{-1})$	$1.79 \times 10^{-12}$	$6.64 \times 10^{-12}$
$M_{m1}$ (%)	0.06	0.58
$M_{m2}$ (%)	0.48	0.42
$M_m$ (%)	0.54	1.00

Figure 4 indicates that water diffuses into the GF/E191 XO/SA specimens at a faster rate with the specimens gaining more mass versus the GF/E188 XO samples. This aligns with material data sheets for the unreinforced acrylic resins that show unreinforced E191 XO/SA reaches a higher percentage mass increase after 7 days at 23°C compared to unreinforced E188 XO, tested as per ISO 62, as displayed in Tab. 1 [27, 28].

Davies et al. found that unreinforced Elium® samples displayed Fickian behaviour. However, when the same resin was reinforced with glass or carbon fibres, evidence of non-Fickian behaviour was observed, suggesting that an additional diffusion mechanism was taking place as well as water entering the resin [22]. As outlined in Sect. 1, diffusion parameters are dependent on multiple factors including resin chemistry, curing conditions, number and location of voids [22, 30]. When evaluating the results of the two diffusion processes occurring simultaneously using a Dual Fickian model, it can be seen that  $D_{z1}$  is a faster process compared to  $D_{z2}$  for both sets of material specimens, as shown in Tab. 2, aligning with Bel Haj Frej et al.'s suggestion that anomalous water uptake can be separated into a 'fast' and 'slow' process [36]. Devine et al. determined a  $D_z$  of  $1.81 \times 10^{-12}$ m<sup>2</sup>s<sup>-1</sup> for GF/Elium<sup>®</sup> 188 O samples when submerged in seawater for 5 months at 50°C, with samples showing evidence of Fickian behaviour [18]. The  $D_{z2}$  values found in this study are of a similar magnitude, with the GF/E191 XO/SA samples experiencing a quicker rate of diffusion, 6.64×10<sup>-12</sup> m<sup>2</sup>s<sup>-1</sup>, compared to GF/E188 XO, 1.79×10<sup>-12</sup> m<sup>2</sup>s<sup>-1</sup>. Interestingly the two material groups in this work reach similar moisture content levels through the second diffusion process, with  $M_{m2}$  values of 0.48% and 0.42% for the GF/E188 XO and GF/E191 XO/SA samples respectively, despite GF/E191 XO/SA having a higher overall

The calculated values from the first diffusion process show a quicker diffusion rate for GF/E188 XO compared to GF/E191 XO/SA, with values of  $1.02 \times 10^{-9}$  m<sup>2</sup>s<sup>-1</sup> and  $1.30 \times 10^{-10}$  m<sup>2</sup>s<sup>-1</sup>. However, the moisture content associated with this diffusion process,  $M_{m1}$ , is significantly different, with GF/E188 XO only reaching 0.06% and GF/E191 XO/SA increasing to 0.58%. It

is acknowledged that there is a greater range in values between the four specimens for the GF/E191 XO/SA samples, which will be discussed further in Sect. 3.1.

#### 3.1 Data Range

The percentage mass increase values used for analysis in this work are the average of the four samples for each material group at each weighing interval. Figure 4 displays the minimum and maximum values recorded, showing a greater range in recorded values for GF/E191 XO/SA. From the average values for GF/E191 XO/SA, the material appears to exhibit Fickian behaviour. However, it is evident that the maximum value is continuing to increase after initially reaching a plateau, whereas the minimum value appears to be decreasing after 2250  $\sqrt{s}$ , suggesting leaching. When evaluating the percentage mass increase values for the individual specimens, the behaviour is split, with two samples following the profile of the maximum values and two samples the minimum. For both material groups, the samples showing the highest percentage mass increase were taken from the inlet end of each laminate, suggesting that one of the mechanisms responsible for diffusion is related to a difference in microstructure due to location within the laminate. This appears to have a stronger influence than the delamination damage caused by water jet cutting when preparing the samples. It is worth noting that some difference in quality and microstructure throughout thick-section laminates is unsurprising due to the associated manufacturing challenges outlined in Sect. 2.3.

Fitting Dual Fickian models to the dataset of each sample allows calculation of individual  $M_m$  values. For the GF/E188 XO samples, the average  $M_m$  from the four individual fits was determined to be 0.54%, with a standard deviation of 0.02%. The four individual fits for the GF/E191 XO/SA samples resulted in an average  $M_m$  of 1.13%, with a standard deviation of 0.65%. This highlights that the GF/E191 XO/SA specimens are behaving inhomogeneously, showing differentiated behaviour making direct comparison between the two materials complex. The overall  $M_m$  values of 0.54% and 1.00% for GF/E188 XO and GF/E191 XO/SA, respectively, displayed in Tab. 2, were calculated using the mean data set. The values calculated using the two different methods therefore align for E188 XO but disagree for E191 XO/SA.

The experimental results and literature considered indicate that two diffusion mechanisms are occurring in each set of material samples, albeit with different coefficients. Root cause analysis of these different processes is considered outside of the scope of this paper and will be investigated in future work, discussed further in Sect. 3.2.

## 3.2 Longer-term Assessment and Future Work

This paper presents results for the first 10 years of an ongoing simulated 20-year period, reflecting the target design lifetime of tidal turbine blades. The full 20-year data set will ultimately be assessed using Fickian and Dual Fickian diffusion models, determining which has a lower SSE, as was performed for the 10-year data period considered in this work. It is anticipated that the Dual Fickian model will still yield lower SSE values and further work is planned to investigate potential causes for the

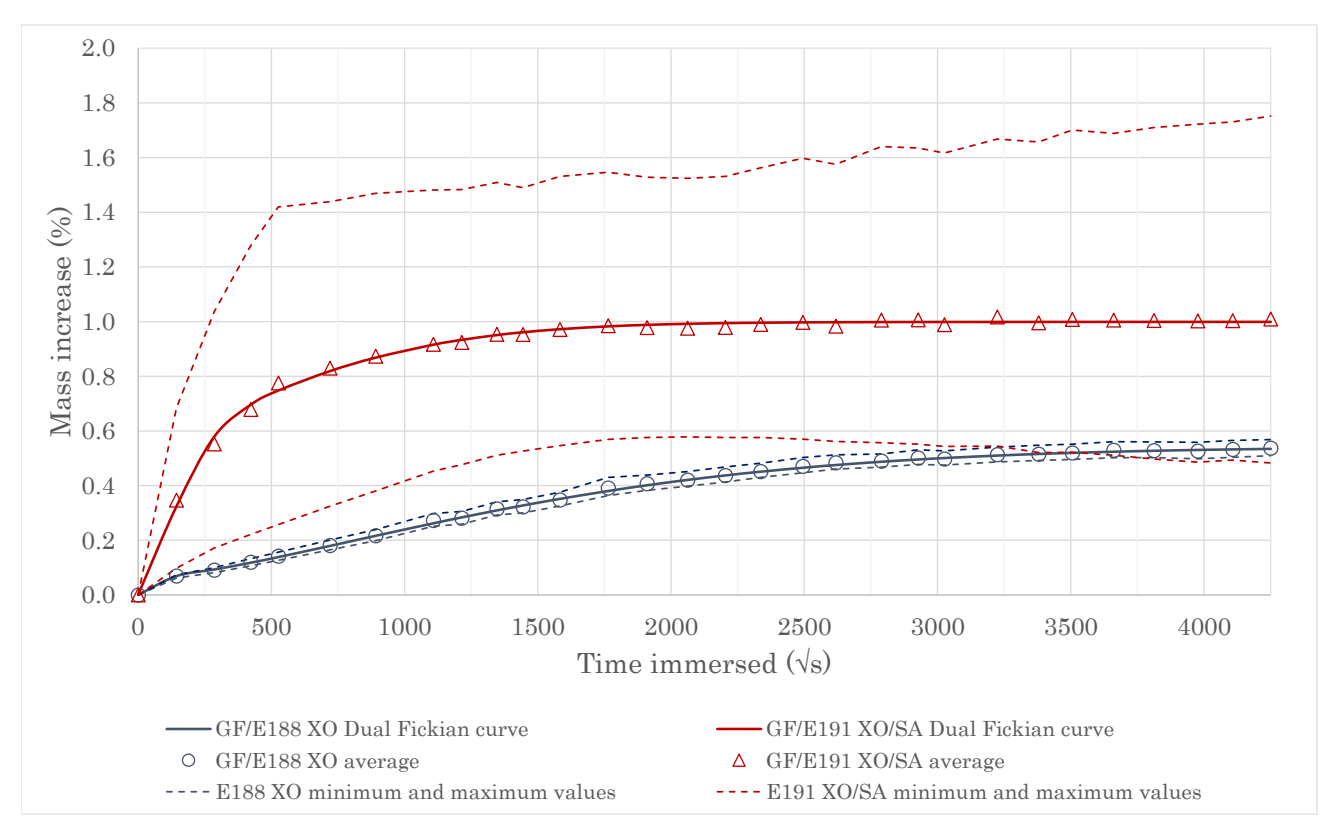


FIGURE 4: WATER ABSORPTION CURVES FOR GF/E188 XO AND GF/E191 XO/SA SAMPLES AT 55°C. CURVES OF BEST FIT FOR EACH DATA SET HAVE BEEN CALCULATED USING A DUAL FICKIAN DIFFUSION MODEL.

two diffusion processes occurring. Longer-term data will enable more in-depth analysis of the water uptake of both materials, particularly for unusual results such as the differing behaviours of the GF/E191 XO/SA samples.

X-ray imaging was used to visually assess the microstructure of samples before immersion. Three specimens of each material were sent for imaging prior to immersion. For each group, the central portion of all three samples was scanned as well as the delaminated corner for one of the affected samples to assess the damage from water jet cutting. This work will be repeated at the end of the 20-year test period, scanning the same areas and enabling direct visual comparison of the microstructure before and after water ageing. Images of the samples before immersion will also be utilised when determining the reason for two diffusion processes.

#### 4. CONCLUSION

This paper aimed to evaluate the long-term behaviour of two acrylic-based, thick-section FRCs in seawater through accelerated ageing testing, forming part of an assessment of their suitability for tidal turbine blade manufacture. Four samples of both GF/Elium<sup>®</sup> 188 XO and GF/Elium<sup>®</sup> 191 XO/SA composites were immersed at 55°C for 7 months to simulate 10 years of submersion. Both materials reached saturation within the test period but demonstrated aspects of non-Fickian behaviour. Fitting a Dual Fickian model provided insights into two simultaneous diffusion processes occurring in each material. The GF/Elium<sup>®</sup> 191 XO/SA composite reached saturation significantly faster than

its counterpart, with a higher total percentage mass increase of 1.00% compared to 0.54%. However, the standard deviation of these results was found to be 0.65% and 0.02% respectively. Given the timeline of the study, these results provide an indication of the diffusion behaviour of the materials assessed but should not be considered conclusive. Nevertheless, there is evidence of a complex relationship between the materials, manufacturing, resulting microstructure, and diffusion behaviour, which should be the subject of further studies.

#### **ACKNOWLEDGEMENTS**

The authors are grateful to EPSRC and NERC for funding for the Industrial CDT for Offshore Renewable Energy (EP/S023933/1) [I.L.M.S]; financial support from the School of Engineering, University of Edinburgh through an Elizabeth Georgeson Fellowship [W.O.];  $\mu$ -VIS X-Ray Imaging Centre at University of Southampton for funding and conducting the imaging studies (EP/T02593X/1). The authors would like to thank Arkema GRL, France; Professor Dipa Ray and Johns Manville for providing material samples used in this research.

### **DECLARATION OF CONFLICTING INTERESTS**

The authors declare that they have no known competing financial interests or personal relationships that could have appeared to influence the work reported in this paper.

#### **REFERENCES**

- [1] Coles, Daniel, Angeloudis, Athanasios, Greaves, Deborah, Hastie, Gordon, Lewis, Matthew, MacKie, Lucas, McNaughton, James, Miles, Jon, Neill, Simon, Piggott, Matthew, Risch, Denise, Scott, Beth, Sparling, Carol, Stallard, Tim, Thies, Philipp, Walker, Stuart, White, David, Willden, Richard and Williamson, Benjamin. "A review of the UK and British Channel Islands practical tidal stream energy resource." *Proceedings of the Royal Society A: Mathematical, Physical and Engineering Sciences* Vol. 477 No. 2255 (2021): p. 20210469. DOI 10.1098/rspa.2021.0469.
- [2] Department for Business, Energy & Industrial Strategy. "Digest of UK Energy Statistics (DUKES) 2024." https://assets.publishing.service.gov.uk/media/66a7e14da3c2a28abb50d922/DUKES\_2024\_Chapters\_1-7.pdf (2024).
- [3] Walker, S. and Thies, P. R. "A review of component and system reliability in tidal turbine deployments." *Renewable and Sustainable Energy Reviews* Vol. 151 (2021): p. 111495. DOI 10.1016/j.rser.2021.111495.
- [4] Jaksic, Vesna, Ó Brádaigh, Conchúr M. and Wallace, Finlay. "Upscaling of Tidal Turbine Blades: Glass or Carbon Fibre Reinforced Polymers?" *12th European Wave and Tidal Energy Conference (EWTEC)*: pp. 1–5. 2017.
- [5] Finnegan, William, Allen, Ronan, Glennon, Conor, Maguire, James M., Flanagan, Michael and Flanagan, Tomas. "Manufacture of High-Performance Tidal Turbine Blades Using Advanced Composite Manufacturing Technologies." *Applied Composite Materials* Vol. 28 No. 6 (2021): pp. 2061–2086. DOI 10.1007/s10443-021-09967y.
- [6] Chen, Junlei, Wang, Jihui and Ni, Aiqing. "Recycling and reuse of composite materials for wind turbine blades: An overview." *Journal of Reinforced Plastics and Composites* Vol. 38 No. 12 (2019): pp. 567–577. DOI 10.1177/0731684419833470.
- [7] Carnicero, Rafael, Cano, Luis and Cruz, Ignacio. "Lessons learned from the sustainable recycling process of a wind blade made with a new thermoplastic resin." *Journal of Physics: Conference Series* Vol. 2767 (2024): p. 072008. DOI 10.1088/1742-6596/2767/7/072008.
- [8] Leon, Mishnaevsky Jr. "Recycling of wind turbine blades: Recent developments." Current Opinion in Green and Sustainable Chemistry Vol. 39 (2023): p. 100746. DOI 10.1016/j.cogsc.2022.100746.
- [9] Kumar, Vishal, Elen, Muthu, Sushmita, Kumari, Overman, Nicole R., Nickerson, Ethan, Murdy, Paul, Presuel-Moreno, Francisco and Fifield, Leonard S. "Hygrothermal aging and recycling effects on mechanical and thermal properties of recyclable thermoplastic glass fiber composites." *Polymer Composites* Vol. 0 (2024): pp. 1–18. DOI 10.1002/pc.29242.
- [10] Obande, Winifred, Mamalis, Dimitrios, Ray, Dipa, Yang, Liu and Ó Brádaigh, Conchúr M. "Mechanical and thermomechanical characterisation of vacuum-infused thermoplastic- and thermoset-based composites." Ma-

- *terials & Design* Vol. 175 (2019): p. 107828. DOI 10.1016/j.matdes.2019.107828.
- [11] Bhudolia, Somen K., Joshi, Sunil C., Bert, Anthony, Yi Di, Boon, Makam, Raama and Gohel, Goram. "Flexural characteristics of novel carbon methylmethacrylate composites." *Composites Communications* Vol. 13 (2019): pp. 129–133. DOI doi.org/10.1016/j.coco.2019.04.007.
- [12] Maguire, James M., Simacek, Pavel, Advani, Suresh G. and Ó Brádaigh, Conchúr M. "Novel epoxy powder for manufacturing thick-section composite parts under vacuum-bag-only conditions. Part I: Through-thickness process modelling." *Composites Part A: Applied Science and Manufacturing* Vol. 136 (2020): p. 105969. DOI 10.1016/j.compositesa.2020.105969.
- [13] Walker, Stuart R.J. and Thies, Philipp R. "A life cycle assessment comparison of materials for a tidal stream turbine blade." *Applied Energy* Vol. 309 (2022): p. 118353. DOI 10.1016/j.apenergy.2021.118353.
- [14] Noble, Donald R., Grattan, Kristofer and Jeffrey, Henry. "Assessing the Costs of Commercialising Tidal Energy in the UK." *Energies* Vol. 17 No. 9 (2024): p. 2085. DOI 10.3390/en17092085.
- [15] Murray, Robynne E., Beach, Ryan, Barnes, David, Snowberg, David, Berry, Derek, Rooney, Samantha, Jenks, Mike, Gage, Bill, Boro, Troy, Wallen, Sara and Hughes, Scott. "Structural validation of a thermoplastic composite wind turbine blade with comparison to a thermoset composite blade." *Renewable Energy* Vol. 164 (2021): pp. 1100–1107. DOI 10.1016/j.renene.2020.10.040.
- [16] Nixon-pearson, Oliver, Greaves, Peter, Mamalis, Dimitrios and Stevenson, Lewis. "WP4 – D1.1. Wind Turbine Blades Design and Manufacturing, Current State-of-the-Art Literature Review." Technical report no. ORE Catapult. 2022.
- [17] Obande, Winifred, Ó Brádaigh, Conchúr M. and Ray, Dipa. "Continuous fibre-reinforced thermoplastic acrylicmatrix composites prepared by liquid resin infusion – A review." *Composites Part B: Engineering* Vol. 215 (2021): p. 108771. DOI 10.1016/j.compositesb.2021.108771.
- [18] Devine, Machar, Bajpai, Ankur, Obande, Winifred, Ó Brádaigh, Conchúr M. and Ray, Dipa. "Seawater ageing of thermoplastic acrylic hybrid matrix composites for marine applications." *Composites Part* B: Engineering Vol. 263 (2023): p. 110879. DOI 10.1016/j.compositesb.2023.110879.
- [19] Kennedy, C. R., Leen, S. B. and Ó Brádaigh, C. M. "Immersed Fatigue Performance of Glass Fibre-Reinforced Composites for Tidal Turbine Blade Applications." *Journal* of Bio- and Tribo-Corrosion Vol. 2 No. 2 (2016): pp. 1–10. DOI 10.1007/s40735-016-0038-z.
- [20] Tual, N, Carrere, N and Davies, Peter. "Characterization of sea water ageing effects on mechanical properties of carbon/epoxy composites for tidal turbine blades." 20th International Conference on Composite Materials Copenhagen: pp. 1–12. 2015.
- [21] Gargano, A., Galos, J. and Mouritz, A. P. "Importance of fibre sizing on the seawater durability of carbon fibre

- laminates." *Composites Communications* Vol. 19 (2020): pp. 11–15. DOI 10.1016/j.coco.2020.02.002.
- [22] Davies, Peter, le gac, pierre yves and Gall, M. "Influence of Sea Water Aging on the Mechanical Behaviour of Acrylic Matrix Composites." *Applied Composite Materials* Vol. 24 (2017): pp. 97–111. DOI 10.1007/s10443-016-9516-1.
- [23] Davies, Peter, Germain, Grégory, Gaurier, Benot, Boisseau, Amlie and Perreux, Dominique. "Evaluation of the durability of composite tidal turbine blades." *Philosophical transactions. Series A, Mathematical, physical, and engineering sciences* Vol. 371 (2013): p. 20120187. DOI 10.1098/rsta.2012.0187.
- [24] Alam, Parvez, Robert, Colin and Ó Brádaigh, Conchúr M. "Tidal turbine blade composites - A review on the effects of hygrothermal aging on the properties of CFRP." *Composites Part B: Engineering* Vol. 149 (2018): pp. 248–259. DOI 10.1016/j.compositesb.2018.05.003.
- [25] Han, Ning, Baran, Ismet, Zanjani, Jamal Seyyed Monfared, Yuksel, Onur, An, LuLing and Akkerman, Remko. "Experimental and computational analysis of the polymerization overheating in thick glass/Elium® acrylic thermoplastic resin composites." *Composites Part B: Engineering* Vol. 202 (2020): p. 108430. DOI 10.1016/j.compositesb.2020.108430.
- [26] Arkema. "Elium<sup>®</sup> Brochure 2024 [online]." https://www.arkema.com/global/en/products/product-finder/product-range/incubator/elium\_resins/ (2024).
- [27] Arkema. "Elium® TDS 188 XO 2023 (online)." https://www.arkema.com/global/en/contact/gated-content-request/ (2023).
- [28] Arkema. "Elium® TDS 191 XO/SA 2023 (online)." https://www.arkema.com/global/en/contact/gated-content-request/ (2023).
- [29] Rajak, Dipen Kumar, Wagh, Pratiksha H. and Linul, Emanoil. "Manufacturing technologies of carbon/glass fiber-reinforced polymer composites and their properties: A review." *Polymers* Vol. 13 No. 21 (2021): p. 3721. DOI 10.3390/polym13213721.
- [30] ASTM International. "Standard Test Method for Moisture Absorption Properties and Equilibrium Conditioning of Polymer Matrix Composite Materials." Technical Report No. ASTM D5229/D5229M-20., West Conshohocken, PA. 2020. DOI 10.1520/D5229 D5229M-20.
- [31] Davies, Peter. "Towards More Representative Accelerated Aging of Marine Composites." Advances in Thick Section Composite and Sandwich Structures. Springer International Publishing (2020): pp. 507–527. DOI 10.1007/978-3-030-31065-3 17.
- [32] Maguire, James M., Koutsos, Vasileios and Ray, Dipa. "Vacuum-infused thermoplastic fibre-metal laminates – Advances in bonding and recycling." *Materials To-day Communications* Vol. 37 (2023): p. 10691. DOI 10.1016/j.mtcomm.2023.106961.

- [33] Kennedy, Ciaran R., Jaksic, Vesna, Leen, Sean B. and Ó Brádaigh, Conchúr M. "Fatigue life of pitch- and stall-regulated composite tidal turbine blades." *Renewable Energy* Vol. 121 (2018): pp. 688–699. DOI 10.1016/j.renene.2018.01.085.
- [34] LeBlac, James, Gauch, Erin, Javier, Carlos and Shukla, Arun. "The Response of Composite Materials Subjected to Underwater Explosive Loading: Experimental and Computational Studies." *Advances in Thick Section Composite and Sandwich Structures*. Springer International Publishing (2020): pp. 43–83. DOI 10.1007/978-3-030-31065-3\_2.
- [35] Cocaud, Julie, Célino, Amandine, Fréour, Sylvain and Jacquemin, Frédéric. "Towards a method for the identification of water diffusion parameters in polymers and composites." *ECCM 2018 18th European Conference on Composite Materials*: pp. 1–8. 2018.
- [36] Bel Haj Frej, Haithem, Léger, Romain, Perrin, Didier and Ienny, Patrick. "A Novel Thermoplastic Composite for Marine Applications: Comparison of the Effects of Aging on Mechanical Properties and Diffusion Mechanisms." *Applied Composite Materials* Vol. 28 (2021): pp. 899–922. DOI 10.1007/s10443-021-09903-0.
- [37] Purnell, P., Cain, J., van Itterbeeck, P. and Lesko, J. "Service life modelling of fibre composites: A unified approach." *Composites Science and Technology* Vol. 68 No. 15 (2008): pp. 3330–3336. DOI 10.1016/j.compscitech.2008.08.026.

# APPENDIX A. ACCELERATION FACTOR CALCULATION

Long-term exposure of a material to seawater can be assessed using accelerated ageing, where increasing the water temperature accelerates the movement of moisture by diffusion into the material, enabling a short period of ageing at a higher test temperature to be equated to a longer period of exposure at a lower service temperature [23, 31, 33, 37]. Assuming an Arrhenius dependency, the diffusion rate  $(k_d)$  varies with temperature, (T):

$$k_d = k_0 e^{-\frac{E_a}{RT}} \tag{4}$$

where  $k_0$  is the reference diffusion rate coefficient,  $E_a$  is the activation energy, R is the universal gas constant (8.3145 kJ kmol<sup>-1</sup>K<sup>-1</sup>) and T is the temperature (K). An acceleration factor  $(AF_{T,S})$  achieved using a higher test temperature  $(T_T)$  with respect to a lower service temperature  $(T_S)$  is defined by [33, 37]:

$$AF_{T,S} = e^{-\left[\frac{E_a}{R}\left(\frac{1}{T_T} - \frac{1}{T_S}\right)\right]}$$
 (5)

The  $E_a$  for this study is assumed to be 48.1 kJ kmol<sup>-1</sup>, calculated using Eqn, 4 and diffusion coefficients for unreinforced acrylic resin at three different temperatures determined by Davies et al [22].  $T_S$  was set as 9°C, and consequently, 55°C was chosen for  $T_T$ . Further reasoning behind this decision is outlined in Sect. 2.4.